Fluorescence Lifetimes of Drusen in Age-Related Macular Degeneration

Chantal Dysli, Rahel Fink, Sebastian Wolf, and Martin S. Zinkernagel

Department of Ophthalmology, Inselspital, Bern University Hospital, Department for BioMedical Research, University of Bern, Bern, Switzerland

Correspondence: Martin S. Zinkernagel, Bern University Hospital, University of Bern, 3010 Bern, Switzerland; m.zinkernagel@gmail.com.

Submitted: May 7, 2017
Accepted: August 4, 2017

Citation: Dysli C, Fink R, Wolf S, Zinkernagel MS. Fluorescence lifetimes of drusen in age-related macular degeneration. *Invest Ophthalmol Vis Sci*. 2017;58:4856–4862. DOI: 10.1167/iovs.17-22184

Purpose. The purpose of this study was to characterize fundus autofluorescence lifetimes of retinal drusen in patients with AMD.

Methods. Patients with AMD and retinal drusen and healthy controls of similar age were examined. A fluorescence lifetime imaging ophthalmoscope was used. Retinal autofluorescence was excited using a 473-nm pulsed laser, and fundus autofluorescence lifetimes of the central retina (30°) were measured in two distinct spectral channels (short: 498 to 560 nm [SSC]; long: 560 to 720 nm [LSC]). Mean retinal autofluorescence lifetimes, corresponding fundus autofluorescence intensity images, spectral domain optical coherence tomography, color fundus images, and clinical data were investigated. Patients were analyzed in two distinct groups (soft drusen and reticular pseudodrusen) and compared with control subjects.

Results. Sixty-four eyes of 64 patients with AMD and retinal drusen (age: mean ± SD, 78 ± 8.5 years; range, 59 to 94 years) were investigated and compared with a control group of 20 age-matched healthy subjects. Mean retinal autofluorescence lifetimes in patients with AMD was significantly prolonged compared with the healthy control eyes (mean ± SEM: SSC, 486 ± 18 vs. 332 ± 11 ps, $P < 0.0001$; LSC: 493 ± 9 vs. 382 ± 17 ps, $P < 0.0001$). Areas of drusen featured a wide range of fluorescence lifetime values. Long lifetimes were identified in areas of atrophy and in areas of intraretinal hyperreflective deposits. Short lifetimes corresponded to deposits within the photoreceptor outer segment band.

Conclusions. Mean retinal autofluorescence lifetimes in AMD patients are significantly prolonged. Intraretinal deposits cause prolonged lifetimes, whereas deposits in the area of the outer photoreceptor segments lead to short fluorescence lifetimes.

Keywords: fluorescence lifetimes, fundus autofluorescence, retinal imaging, FLIO, age-related macular degeneration, AMD, deposits, drusen

AMD is caused by age-related metabolic disorders in the retina, which leads to thickening of the Bruch membrane with calcifications, basal laminar deposits, and appearance of drusen. The predominant symptom is progressive central vision loss. The prevalence of advanced AMD is estimated to increase from 2.2% in 65-year-old patients to more than 21% in patients older than 90 years.[1] Various risk factors have been identified, including age, sex, arterial hypertension, arteriosclerosis, elevated serum lipids, smoking, alcohol abuse, exposure to UV light, and various genetic factors.[2–6]

The hallmark of early AMD is the presence of retinal drusen, which can be classified into soft drusen of various sizes (small, medium, large), hard drusen, cuticular drusen, crystalline drusen, and reticular pseudodrusen.[4,7] In the biomicroscopic fundus examination, drusen are seen as discrete, yellow-white punctuate elevations. Retinal drusen are focal deposits of extracellular debris located between the basal lamina of the RPE and the inner collagenous layer of the Bruch membrane and are mainly concentrated within the posterior pole. The largest single component of drusen is lipid. Other elements are carbohydrates, zinc, and nearly 150 proteins, including vitronectin and apolipoproteins E and B.[8] Most of the components are photoreceptor- and mitochondria-derived proteins and thus involved in the lipofuscin metabolism.[9] Hard drusen have a diameter of less than 30 to 63 μm and their borders are very confined. Soft drusen typically have a diameter of 63 μm to more than 125 μm, and their outer borders may be confluent. In fluorescein angiography (FA), soft drusen are usually minimally hyperfluorescent in late stages. Histopathologic investigations showed that soft drusen are mounds basal to the RPE basement membrane containing lipoprotein-derived debris and thus can disturb the architecture of the RPE.

Reticular pseudodrusen, on the other hand, are located in the subretinal space rather than being sub-RPE. They are mainly distributed perifoveally, and their size ranges from 25 μm to more than 125 μm. According to postmortem studies, reticular pseudodrusen share superficial ultrastructural and compositional similarities with soft drusen.[4,10] On optical coherence tomography (OCT) scans, reticular pseudodrusen are visible as granular hyperreflective deposits between the RPE and the inner segment ellipsoid lines.[4,8] They can be large enough to break through the ellipsoid line and disturb or shorten the overlying photoreceptors and form conical accumulations that can breach the external limiting membrane. Reticular pseudodrusen are especially visible in near infrared reflectance imaging and may appear hypofluorescent in fluorescein angiography.[4]

Small drusen (<63 μm) can be a sign of normal retinal aging changes and are not associated with increased risk of late AMD

development. However, medium drusen (63 to 125 μm) should be considered early AMD. Intermediate AMD is characterized by large drusen (>125 μm) and/or pigmentary abnormalities associated with at least medium drusen. Neovascular AMD and/or geographic atrophy are signs of late AMD. Five-year risks of progressing to late AMD are estimated to increase approximately 100-fold depending on the actual stage of AMD, ranging from a 0.5% 5-year risk for normal aging changes to a 50% risk for the highest-intermediate AMD risk group.[2,11,12]

Fluorescence lifetime imaging ophthalmoscopy (FLIO) can identify early retinal changes in degenerative retinal diseases and has been shown to provide not only information about the integrity of the RPE but of the photoreceptors as well.[13–22] FLIO measures the lifetime time span of naturally occurring retinal fluorophores on excitation with a blue laser light impulse. Fluorescence lifetimes are specific for each molecule. They are known to be independent of the fluorescence intensity and are influenced by the local metabolic environment.[23]

First studies measuring fluorescence lifetimes in AMD have shown prolonged lifetimes compared to healthy subjects.[24,25] Detailed analysis of drusen as the hallmark of early and intermediate AMD, and identification of early metabolic and structural changes in AMD could help to identify patients at risk and may be helpful for predicting disease development and progression.

Methods

All participants were recruited from the outpatient clinic of the department of ophthalmology at the University Hospital in Bern, Switzerland. The study protocol was approved by the local ethics committee and is in accordance with the Declaration of Helsinki and the International Ethical Guidelines for Biomedical Research involving Human Subjects (Council for International Organizations of Medical Sciences [CIOMS]). The study is registered at ClinicalTrials.gov (NCT01981148) with the title "Measurement of Retinal Autofluorescence with a Fluorescence Lifetime Imaging Ophthalmoscope." Informed written consent was obtained from all participants before study entry.

Subjects and Procedures

A standardized sequence of investigations was performed for every patient, which included measurement of best-corrected visual acuity (Early Treatment Diabetic Retinopathy Study [ETDRS] letters)[26] and measurement of intraocular pressure using air tonometry as a noncontact system to avoid corneal staining with fluorescein. After maximal pupil dilation with tropicamid 0.5% and phenylephrine hydrochloride 2.5%, a general ophthalmic examination by a retinal specialist was performed. Eyes with ocular pathologies besides AMD such as media opacities and other retinal pathologies were excluded to avoid potential imaging artifacts. Multimodal imaging of the central 30° retinal field was performed including optical coherence tomography (OCT) and fundus autofluorescence (FAF) measurement (Heidelberg Spectralis HRA+OCT; Heidelberg Engineering, Heidelberg, Germany), fundus color imaging (Zeiss FF 450plus; Carl Zeiss Meditec, Jena, Germany), and fluorescence lifetime imaging ophthalmoscopy (Heidelberg Engineering).

Stages of AMD were classified as follows: early AMD with small to medium drusen, intermediate stage with large (>125 μm) more confluent drusen and/or pigmentary abnormalities, and late AMD with geographic atrophy or exudative AMD with intraretinal fluid as sign of retinal neovascularisation.[11] The existing drusen were divided into soft drusen and reticular pseudodrusen according to their appearance in OCT and the corresponding infrared image.[4] Data were further analyzed considering the lens status (phakic or pseudophakic).

Fluorescence Lifetime Imaging Ophthalmoscope and Image Analysis

Fluorescence lifetime data were acquired using a fluorescence lifetime imaging ophthalmoscope based on a Heidelberg retina angiograph (HRA) Spectralis system (Heidelberg Engineering). The FLIO system and its technical background are described in previous publications including detailed laser safety calculations.[13,14]

Retinal autofluorescence was excited using a 473-nm pulsed laser raster-scanning the central fundus (30°) with a repetition rate of 80 MHz. The laser exposure is well below the limits set by the International Electrotechnical Commission.[27] Emitted photons were detected by highly sensitive hybrid photon-counting detectors (HPM-100-40; Becker&Hickl, Berlin, Germany) and registered by time-correlated single-photon counting (TCSPC) modules (SPC-150; Becker&Hickl). Photons were separately detected in two channels according to their wavelength: in a short spectral channel (wavelengths 498 to 560 nm, SSC) and in a long spectral channel (560 to 720 nm, LSC). A minimum of 1000 photons per pixel was recorded within the macular center in both channels. In parallel, eye movements were tracked by an inbuilt infrared reflectance camera to ensure correct allocation of detected photons within the 256 × 256-pixel frame.

Recorded fluorescence lifetime data were analyzed using SPCImage 5.4 software (Becker&Hickl). A binning factor of one was applied, averaging the photons of an individual pixel point with the directly adjacent pixels to increase the numbers of photons per pixel. A fluorescence decay histogram was generated for every single data point in both spectral channels using a bi-exponential decay function.

The resulting individual lifetime components within the SSC and the LSC were a short (*T1*) and a long (*T2*) decay time with their corresponding relative amplitudes (=relative intensity) $\alpha 1$ and $\alpha 2$, whereby $T1 << T2$ and $\alpha 1 >> \alpha 2$.

Of these four components *T1, T2,* $\alpha 1$, and $\alpha 2$, the mean fluorescence lifetime tau mean (*Tm*) can be calculated. It represents the amplitude weighted mean fluorescence decay time per pixel and wavelength channel.

$$T_m = \frac{a_1 * T_1 + a_2 * T_2}{a_1 + a_2} \quad (1)$$

FLIO data was averaged and analyzed using the custom made FLIO reader (ARTORG Center for Biomedical Engineering Research, University of Bern, Bern, Switzerland). A standard ETDRS grid (Circle diameters central area [C] 1 mm, inner ring [IR] 3 mm, outer ring [OR] 6 mm) was used for analysis of individual retinal areas.[13] For analysis of specific regions of interest (ROI), a small circle with 0.2 mm diameter was used.

The primary outcome was the mean fluorescence lifetime *Tm*. Further values of interest were the short (*T1*) and the long (*T2*) lifetime components with the corresponding amplitudes $\alpha 1$ and $\alpha 2$ as the individual components of *Tm*.

Statistical Analysis

For statistical analysis, only data of one eye per patient was used. If applicable, the eye with the better image quality was chosen; otherwise, one eye was selected randomly. Values are shown as mean ± SEM. All statistical analysis was done using Graph Pad Prism version 6 (GraphPad Software, Inc., La Jolla, CA, USA). Data groups were compared using a two-tailed *t*-test

Table. Overview of Patient Characteristics

	No., %	Age, y (Mean ± SD)	Female, y	Male, y	BCVA (Mean ± SD)	Phakic, %	Psudophakic, %
All patients	64	77.9 ± 8.5	40	24	71.3 ± 14.9	39 (61%)	25 (39%)
Soft drusen	30 (47%)	73.2 ± 8.6	19	11	75.7 ± 12.9	20	10
Reticular drusen	34 (53%)	82.3 ± 6.0	21	13	67.4 ± 15.7	19	15
Healthy subjects	20	74.5 ± 8.5	3	17	79.9 ± 9.4	15	5

for parametric data with a confidence interval of 95%. $P < 0.05$ was considered statistically significant.

Results

Sixty-four patients with retinal drusen were included in this study; 62.5% ($n = 40$) were female. The age ranged from 59 to 94 years, with a mean of 78 years (±8.5 SD). Two eyes (3%) had early AMD, 28 eyes (44%) had intermediate AMD, 13 eyes (20%) had dry AMD, and 21 eyes (33%) had exudative AMD; 46.9% ($N = 30$) of the eyes showed predominantly soft drusen, whereas 53.1% ($n = 34$) exhibited mainly reticular pseudodrusen. Thirty-nine percent of the eyes ($n = 25$) were pseudophakic. The mean best-corrected visual acuity was 71 ± 1.9 SEM ETDRS letters (range, 23–93). A control group of 20 eyes of 20 age-matched participants was used (range, 59 to 87 years; mean, 75 years; SD, 8.5; $P = 0.13$). An overview of patient characteristics is provided in the Table.

Fluorescence Lifetimes in Patients With AMD and Retinal Drusen

Mean retinal autofluorescence lifetimes in patients with AMD and reticular pseudodrusen and/or soft drusen were significantly prolonged compared with the healthy control eyes (Fig. 1). In phakic eyes, mean lifetime values ± SEM of the outer ETDRS ring were 613 ± 29 ps compared with 346 ± 13 ps in healthy controls in the SSC, and 545 ±1 7 ps compared with 370 ± 13 ps in the LSC (both $P < 0.0001$). In pseudophakic eyes, mean lifetime values were 404 ± 8 ps compared with 325 ± 15 ps in healthy controls in the SSC ($P = 0.0004$) and 475 ± 9 ps compared with 419 ± 22 ps in the LSC ($P = 0.0145$).

The ROI of drusen and the surrounding retina within the area of the outer ETDRS ring featured a broader range of fluorescence lifetime values. The mean fluorescence lifetimes of reticular pseudodrusen ranged from 325 to 1093 ps with a mean of 554 ps in the SSC and from 349 to 726 ps with a mean of 536 ps in the LSC. The mean fluorescence lifetimes of soft drusen ranged from 311 to 813 ps with a mean of 468 ps in the SSC and from 321 to 650 ps with a mean of 476 ps in the LSC. The mean autofluorescence lifetime within specific ROIs are summarized in Figure 2.

The detailed analysis of individual lifetime components of *Tm* (*T1, T2, α1*, and *α2*; see Methods, Equation 1) did not contribute to a better identification of soft drusen or reticular pseudodrusen.

Correlation of Fluorescence Lifetimes Data With Findings in OCT

Drusen were colocalized using corresponding OCT, IR, FAF, and FLIO images. Soft drusen with subretinal accumulation of hyperreflective material identified in OCT showed distinctively shortened lifetimes compared with the surrounding retina (Fig. 3A). Soft drusen with hyporeflective sub-RPE material did not show fluorescence lifetime differing from the surrounding retina (Figs. 2A, 3A). However, intraretinal hyperreflective deposits led to marked prolongation of lifetimes (Fig. 3B) even in the presence of surrounding short lifetime drusen. Reticular pseudodrusen generally displayed slightly longer lifetimes compared with soft drusen (Fig. 2C).

Distribution Histogram of Fluorescence Lifetime Components

Figure 4 shows a representative example of a two-dimensional (2D) distribution histogram in a patient with short and long mean lifetime deposits. The short lifetime component *T1* (see Equation 1) was in the range of 150 to 350 ps and the long decay component *T2* between 1500 and 2500 ps. Using 2D distribution clouds, areas of prolonged or shortened mean fluorescence lifetimes were visible. Compared with the main retina, deposits with short mean fluorescence lifetime values featured significantly shorter *T1*, whereas drusen with long mean fluorescence lifetimes mainly showed longer lifetime components *T2*. (Figs. 4A, 4B)

Discussion

Autofluorescence lifetime imaging in patients with AMD revealed a generalized prolongation of retinal lifetimes within the ETDRS grid compared with age-matched healthy controls independent of the presence or absence and the type of drusen (soft drusen or reticular pseudodrusen). These data are in keeping with previous studies of FLIO in AMD[24] and ex vivo fluorescence lifetime data of human donor retinal tissue containing extramacular drusen.[28] Our data shows that sub- and intraretinal deposits feature characteristic lifetime patterns that may yield information about their composition and duration of existence. It should be kept in mind that the human lens itself has a long fluorescence lifetime and may therefore influence fluorescence lifetime dynamics of the retina. This is evident from our data, where the differences of mean lifetime between AMD patients and healthy controls were 257 ps in the short wavelength channel for phakic eyes and only 79 ps for pseudophakic eyes. This infers that fluorescence lifetimes are influenced by the fluorescence of the crystalline lens, especially in older patients. However, the trend of lifetime changes between AMD patients and healthy subjects in our study was comparable for phakic and for pseudophakic eyes. For quantitative measurements, it may be useful to incorporate the influence of the human lens for quantification of retinal lifetimes.

The general prolongation of retinal fluorescence lifetime is not surprising in synopsis with results from fluorescence lifetime measurements in other retinal pathologies and progressive age,[16,18,21] and can be explained by accumulation of lipofuscin, as well as progressive remodeling of the retina with possibly increasing content of connective tissue components such as collagen, which have been shown to exhibit long fluorescence lifetimes.[29] Elevated lipofuscin contained in the RPE may precede or coexist with the earliest stages of pathology in AMD.[30] However, in the late stages of AMD, RPE lipofuscin is decreased.

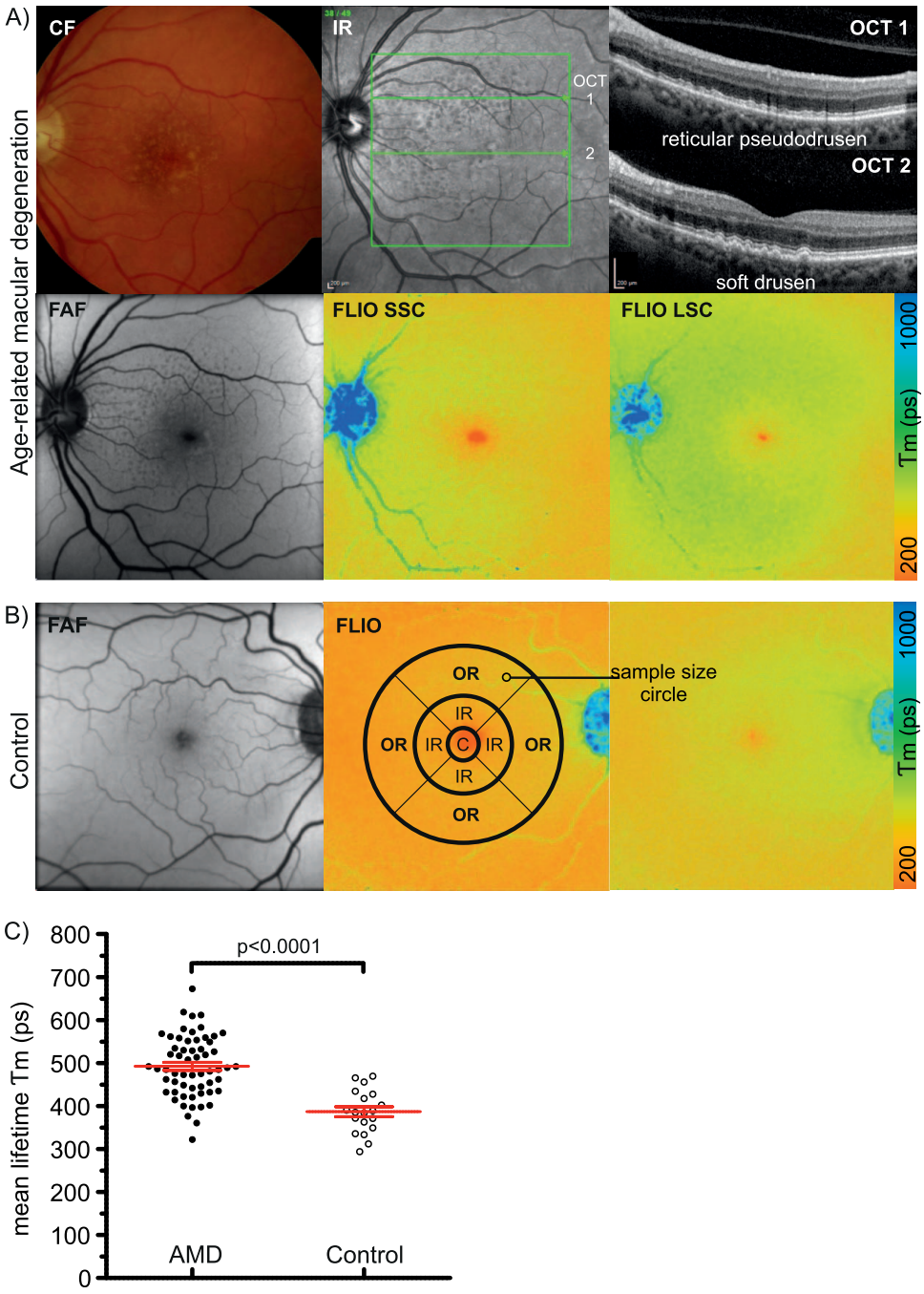

Figure 1. Autofluorescence lifetime imaging (FLIO) in the left eye of a patient with reticular pseudodrusen and soft retinal drusen due to age-related macular degeneration (**A**) and a healthy control eye (**B**). Multimodal imaging with corresponding CF, IR, FAF, and autofluorescence lifetime images (FLIO, short and long spectral channel [SSC = 498 to 560 nm, LSC = 560 to 720 nm]) is shown. (**B**) Healthy control eye with indicated way of data analysis. A standard ETDRS grid (center [diameter; d = 1 mm], inner [d = 3 mm] and the outer [d = 6 mm] ETDRS ring) was used for data averaging. The indicated sample size circle (d = 0.2 mm) was used for analysis of specific regions (ROI). (**C**) Comparison of mean fluorescence lifetimes from the outer ETDRS ring in AMD and healthy control eyes.

Soft drusen, irrespective of the size and height of hyporeflective subretinal deposits in OCT, did not stand out from the surrounding retina in fluorescence lifetime measurements. In autofluorescence intensity imaging, drusen have an extremely variable appearance depending on size and integrity of the overlying RPE and ellipsoid zone. Whereas large and confluent soft drusen may result in hyperfluorescent autofluorescence changes, smaller drusen are often iso-autofluorescent and remain undetected in fundus autofluorescence imaging.

In FLIO, soft drusen did not contrast to the surrounding retinal tissue, and this may be explained either by the absence of fluorescing material within soft drusen, or the absence of autofluorescence for the given excitation wavelength of 473 nm. However, in the presence of intra- or subretinal hyperreflective deposits, as identified in OCT, fluorescence lifetime changes colocalized with soft drusen were observed.

Reticular pseudodrusen represent as small hyperreflectivities in OCT directly on top of the RPE. Depending on the

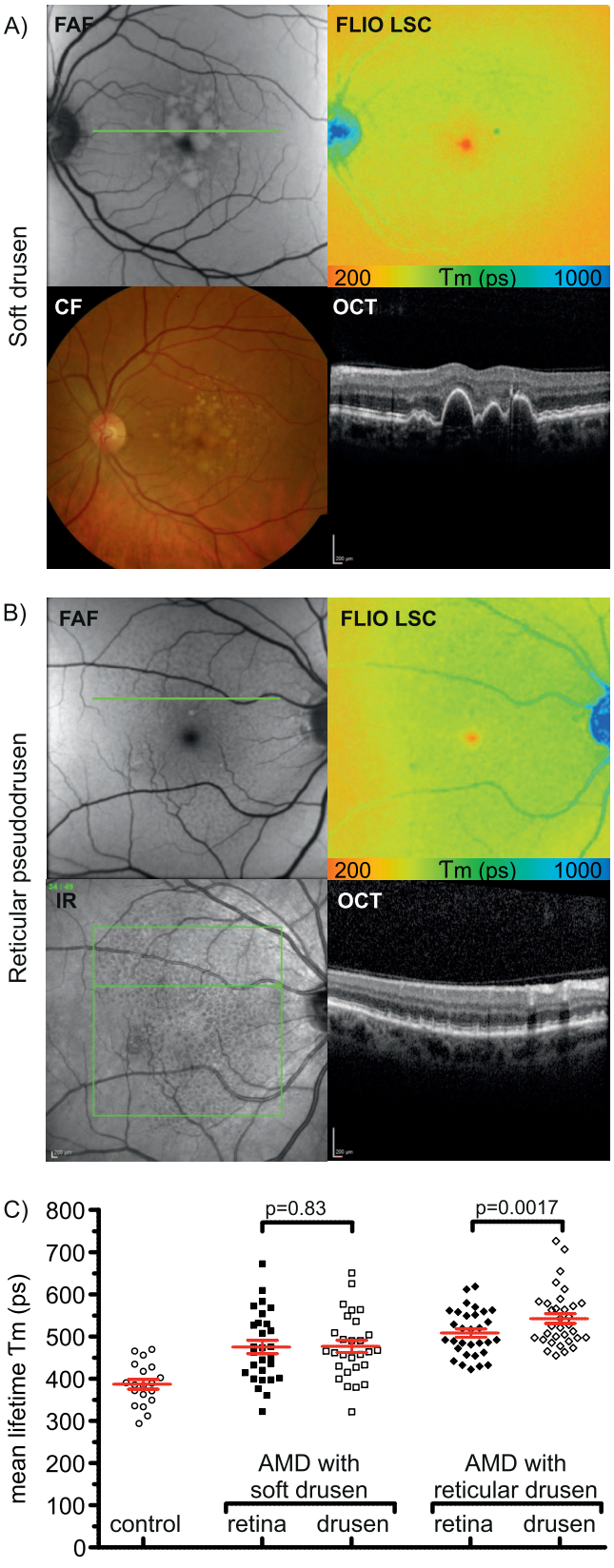

Figure 2. FLIO in soft drusen (**A**) and reticular pseudodrusen (**B**). (**C**) Quantitative analysis of fluorescence lifetimes in the long spectral channel for control eyes and soft drusen respectively reticular pseudodrusen in AMD. FAF, autofluorescence lifetime images (FLIO, long spectral channel LSC = 560 to 720 nm), CF, and OCT of the indicated *green line* in the FAF image.

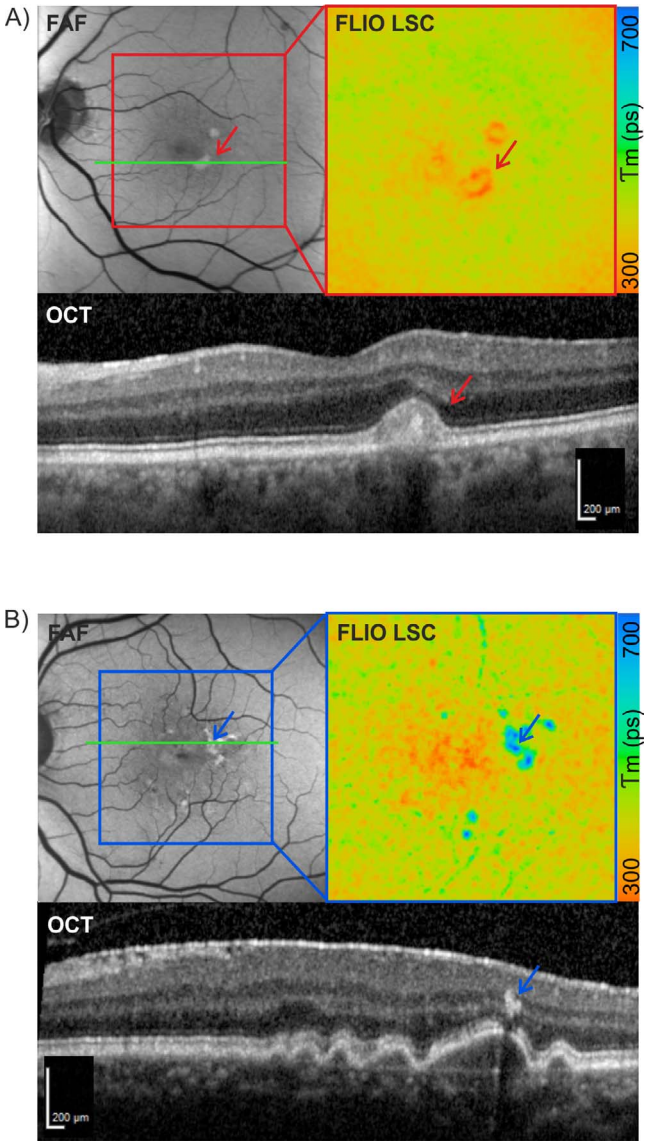

Figure 3. Correlation of fluorescence lifetime findings with OCT. (**A**) Areas of short fluorescence lifetimes (*red*) in FLIO corresponded to hyperfluorescent areas in FAF images and to hyperdense deposits in the photoreceptor outer segment–RPE band in the OCT images. (**B**) Areas of long fluorescence lifetimes (*blue*) in FLIO corresponded to intraretinal hyperreflective deposits overlying a large druse. Soft drusen as seen in OCT did not contrast with the surrounding retina in FLIO. FAF intensity, autofluorescence lifetime images (FLIO, long spectral channel LSC = 560 to 720 nm; color scale, 300 to 700 ps), and OCT of the indicated *green line* in the FAF image.

morphology and integrity of the overlying boundary between the inner segments (ISs) and the outer segments (OSs) of the photoreceptors (IS/OS boundary), reticular pseudodrusen can be classified in four stages.[31] In autofluorescence intensity measurements, reticular pseudodrusen appear as small foci of hypo-autofluorescence surrounded by dispersed hyper-autofluorescence in a reticular pattern. Hypo-fluorescence is likely to result from blockage of RPE fluorescence by overlying reticular pseudodrusen. Despite their subretinal localization, the autofluorescence pattern suggests that these drusen do not contain high contents of bisretinoids.[4] The relative lack of autofluorescence and the small size of these deposits, which are possibly below the resolution of the FLIO device, did not allow identifying individual reticular pseudodrusen with FLIO.

Investigative Ophthalmology & Visual Science

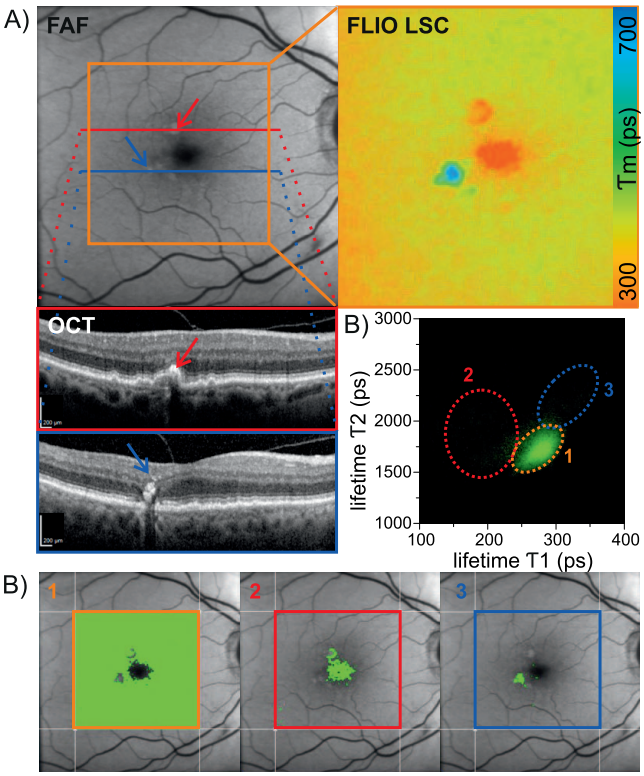

Figure 4. Lifetime distribution histogram in deposits of short and long fluorescence lifetimes. (**A**) FAF intensity, autofluorescence lifetime images (FLIO, long spectral channel LSC = 560 to 720 nm; color scale, 300 to 700 ps), and OCT of the indicated red and blue lines in the FAF image are shown below. (**B**) Lifetime clouds of short and long mean fluorescence lifetimes were clearly identifiable using the 2D histograms (T1 against T2; see Equation 1). Corresponding areas are highlighted in B1–3 below.

Areas of short fluorescence lifetimes in FLIO correlated with hyperdense deposits in the photoreceptor outer segment band and subretinal deposits in our study. Photoreceptor-derived subclinical subretinal deposits after atrophy of the photoreceptors were already proposed by Sarks et al. in 1988.[32] The finding of short retinal fluorescence lifetimes in areas of accumulated or thickened photoreceptor segments is in accordance with our previous studies.[14,17] In Stargardt disease, we identified flecks with very short fluorescence lifetimes and speculated that these represent bisretinoids deriving from the visual cycle. Likewise, areas with elongated outer photoreceptor segments in patients with central serous chorioretinopathy had a marked reduction of fluorescence lifetimes. These shed outer segments containing retinoids such as retinaldehyde adducts and highly polyunsaturated fatty acids.[33] Considering these findings, we speculate that short fluorescence lifetimes found in a subgroup of drusen are an indicator for newly developing drusen with dysfunctional outer segment phagocytosis. Further studies are warranted to confirm this hypothesis.

Long retinal autofluorescence lifetimes can result from retinal atrophy as seen in the area of geographic atrophy.[16] However, long lifetimes were also seen in areas with preserved retinal layer structure. These long lifetime spots corresponded to intraretinal hyperdensities in OCT, which are described as aberrant or migrated dysfunctional RPE cells or cell fragments.[34] The migration of RPE cells is assumed to be facilitated by the prevalence of underlying drusen. To identify the potential of FLIO as a diagnostic tool to record disease development over time and to find early markers to identify patients with progression from an early stage to intermediate or late stages of AMD, follow-up examinations will be crucial. This could provide a baseline for early intervention and drug development to prevent or delay progressive irreversible loss of retinal structure and function.

Conclusions

Retinal autofluorescence lifetimes in AMD were significantly prolonged compared with healthy control eyes. Drusen exhibit variable fluorescence lifetime characteristics not only associated with respective location and concurrent RPE changes. As such, fluorescence lifetime features may change within individual drusen over time and may help to identify newly formed drusen. Longitudinal studies are currently underway to investigate the significance of drusen lifetimes as biomarker for disease progression.

Acknowledgments

The authors thank Joerg Fischer, PhD, Yoshihiko Katayama, PhD, and Kester Nahen, PhD (Heidelberg Engineering GmBH, Heidelberg, Germany), for providing technical assistance for the FLIO device.

Supported by Swiss National Science Foundation Grant 320030_156019 (Bern, Switzerland). The sponsor or funding organization had no role in the design or conduct of this research.

Disclosure: **C. Dysli**, Heidelberg Engineering (S); **R. Fink**, None; **S. Wolf**, Heidelberg Engineering (C, S), Bayer (C), Novartis, (C), Alcon (C), Allergan (C), Roche (C); **M.S. Zinkernagel**, Heidelberg Engineering (S), Bayer (C), Novartis (C, I)

References

1. Wilde C, Poostchi A, Mehta RL, et al. Prevalence of age-related macular degeneration in an elderly UK Caucasian population—The Bridlington Eye Assessment Project: a cross-sectional study. *Eye (Lond)*. 2017;31:1042–1050.
2. Lambert NG, ElShelmani H, Singh MK, et al. Risk factors and biomarkers of age-related macular degeneration. *Prog Retinal Eye Res*. 2016;54:64–102.
3. Korner-Stiefbold U. Age-related macular degeneration (AMD): therapeutic possibilities and new approaches [in German]. *Ther Umsch*. 2001;58:28–35.
4. Khan KN, Mahroo OA, Khan RS, et al. Differentiating drusen: drusen and drusen-like appearances associated with ageing, age-related macular degeneration, inherited eye disease and other pathological processes. *Prog Retinal Eye Res*. 2016;53:70–106.
5. Tomany SC, Wang JJ, Van Leeuwen R, et al. Risk factors for incident age-related macular degeneration: pooled findings from 3 continents. *Ophthalmology*. 2004;111:1280–1287.
6. Zinkernagel MS, Zysset-Burri DC, Keller I, et al. Association of the intestinal microbiome with the development of neovascular age-related macular degeneration. *Sci Rep*. 2017;7:40826.
7. Reim M, Kirchhof B, Wolf S. *Diagnose am Augenhintergrund* [in German]. Stuttgart, Germany: Georg Thieme Verlag; 2004.
8. Spaide RF, Curcio CA. Drusen characterization with multimodal imaging. *Retina*. 2010;30:1441–1454.
9. Schutt F, Ueberle B, Schnolzer M, Holz FG, Kopitz J. Proteome analysis of lipofuscin in human retinal pigment epithelial cells. *FEBS Lett*. 2002;528:217–221.
10. Rudolf M, Malek G, Messinger JD, Clark ME, Wang L, Curcio CA. Sub-retinal drusenoid deposits in human retina: organization and composition. *Exp Eye Res*. 2008;87:402–408.

11. Ferris FL III, Wilkinson CP, Bird A, et al. Clinical classification of age-related macular degeneration. *Ophthalmology*. 2013; 120:844–851.
12. Klein R, Myers CE, Lee KE, et al. Small drusen and age-related macular degeneration: the Beaver Dam Eye Study. *J Clin Med*. 2015;4:424–440.
13. Dysli C, Quellec G, Abegg M, et al. Quantitative analysis of fluorescence lifetime measurements of the macula using the fluorescence lifetime imaging ophthalmoscope in healthy subjects. *Invest Ophthalmol Vis Sci*. 2014;55:2106–2113.
14. Dysli C, Wolf S, Hatz K, Zinkernagel MS. Fluorescence lifetime imaging in stargardt disease: potential marker for disease progression. *Invest Ophthalmol Vis Sci*. 2016;57:832–841.
15. Dysli C, Wolf S, Zinkernagel MS. Fluorescence lifetime imaging in retinal artery occlusion. *Invest Ophthalmol Vis Sci*. 2015;56:3329–3336.
16. Dysli C, Wolf S, Zinkernagel MS. Autofluorescence lifetimes in geographic atrophy in patients with age-related macular degeneration. *Invest Ophthalmol Vis Sci*. 2016;57:2479–2487.
17. Dysli C, Berger L, Wolf S, Zinkernagel MS. Fundus autofluorescence lifetimes and central serous chorioretinopathy [published online ahead of print January 17, 2017]. *Retina*. doi:10.1097/IAE.0000000000001452.
18. Dysli C, Wolf S, Tran HV, Zinkernagel MS. Autofluorescence lifetimes in patients with choroideremia identify photoreceptors in areas with retinal pigment epithelium atrophy. *Invest Ophthalmol Vis Sci*. 2016;57:6714–6721.
19. Sauer L, Schweitzer D, Ramm L, Augsten R, Hammer M, Peters S. Impact of macular pigment on fundus autofluorescence lifetimes. *Invest Ophthalmol Vis Sci*. 2015;56:4668–4679.
20. Sauer L, Peters S, Schmidt J, et al. Monitoring macular pigment changes in macular holes using fluorescence lifetime imaging ophthalmoscopy. *Acta Ophthalmol*. 2017;95:481–492.
21. Schmidt J, Peters S, Sauer L, et al. Fundus autofluorescence lifetimes are increased in non-proliferative diabetic retinopathy. *Acta Ophthalmol*. 2017;95:33–40.
22. Dysli C, Wolf S, Berezin MY, Sauer L, Hammer M, Zinkernagel MS. Fluorescence lifetime imaging ophthalmoscopy [published online ahead of print June 30, 2017]. *Prog Retinal Eye Res*. doi:10.1016/j.preteyeres.2017.06.005.
23. Schweitzer D, Schenke S, Hammer M, et al. Towards metabolic mapping of the human retina. *Microscopy Res Technique*. 2007;70:410–419.
24. Schweitzer D, Quick S, Schenke S, et al. Comparison of parameters of time-resolved autofluorescence between healthy subjects and patients suffering from early AMD [in German]. *Der Ophthalmologe: Zeitschrift der Deutschen Ophthalmologischen Gesellschaft*. 2009;106:714–722.
25. Schweitzer D, Hammer M, Schweitzer F, et al. In vivo measurement of time-resolved autofluorescence at the human fundus. *J Biomed Optics*. 2004;9:1214–1222.
26. Early Treatment Diabetic Retinopathy Study Research Group. Early Treatment Diabetic Retinopathy Study design and baseline patient characteristics. ETDRS report number 7. *Ophthalmology*. 1991;98(5 Suppl):741–756.
27. International Electrotechnical Commission. Safety of laser products - part 1: equipment classification and requirements. In: *IEC 60825-1:2014*. 3rd ed. International Electrotechnical Commission; 2014.
28. Schweitzer D, Gaillard ER, Dillon J, et al. Time-resolved autofluorescence imaging of human donor retina tissue from donors with significant extramacular drusen. *Invest Ophthalmol Vis Sci*. 2012;53:3376–3386.
29. Schweitzer D. Metabolic mapping. In: Holz FG, Spaide RF, eds. *Medical Retina: Essentials in Ophthalmology*. Berlin: Springer-Verlag; 2010:107–123.
30. Solbach U, Keilhauer C, Knabben H, Wolf S. Imaging of retinal autofluorescence in patients with age-related macular degeneration. *Retina*. 1997;17:385–389.
31. Zweifel SA, Spaide RF, Curcio CA, Malek G, Imamura Y. Reticular pseudodrusen are subretinal drusenoid deposits. *Ophthalmology*. 2010;117:303–312.
32. Sarks JP, Sarks SH, Killingsworth MC. Evolution of geographic atrophy of the retinal pigment epithelium. *Eye (Lond)*. 1988; 2(Pt 5):552–577.
33. Warburton S, Southwick K, Hardman R, et al. Examining the proteins of functional retinal lipofuscin using proteomic analysis as a guide for understanding its origin. *Molec Vis*. 2005:1122–1134.
34. Ho J, Witkin AJ, Liu J, et al. Documentation of intraretinal retinal pigment epithelium migration via high-speed ultra-high-resolution optical coherence tomography. *Ophthalmology*. 2011;118:687–693.

Investigative Ophthalmology & Visual Science